Dust and wind formation in low-metallicity AGB-stars

Ch. Helling, T.U. Arndt, E. Sedlmayr
(Zentrum für Astronomie und Astrophysik, TU Berlin,
Hardenbergstraße 36, D-10623 Berlin, Germany)
email: chris@astro.physik.tu-berlin.de, arndt@astro.physik.tu-berlin.de

Introduction

The formation of dust and wind in luminous AGB-stars has been studied so far mainly for solar metallicities. Here, the impact of the dust component for the driving mechanism of the massive outflows and the non-linear coupling to hydro-/thermodynamics lead to the creation of dust induced shock waves, the occurrence of onion-like spatial dust distributions around the star, time-dependent dust size distributions, multi-periodicity, the onset of a super-wind phase. The question remains to which extent these phenomena appear in metal-deficient AGB stars like those of the Large Magellanic Cloud (LMC).

Approach

Time-dependent, spherical symmetric models of carbon-rich dynamical atmospheres of LPVs have been calculated by means of the CHILD-code developed by Fleischer et al. (1992) in an updated version of Helling et al. (2000b). The code solves the coupled equation system of hydrodynamics, radiative transfer, chemistry, and dust formation. Dust nucleation, growth and evaporation are treated by the moment method (Gail & Sedlmayr 1988, Gauger et al. 1990). The composition of the gas is calculated in chemical equilibrium and the interior pulsation of the star is simulated by a sinusoidal variation of the innermost grid point with prescribed period P and velocity amplitude Δu. The initial values are given by the static, dust-free case. The radiative transfer problem is solved in grey approximation (Unno & Kondo 1976, 1977, Hashimoto 1995). The mean gas opacity is approximated by its Planck mean. The dust extinction is adopted either from Gail & Sedlmayr (1985) or Preibisch et al. (1993) (Table 1).

The time-dependent models are completely determined by 4 **stellar parameter**: $T_\star$, $L_\star$, $M_\star$, elemental abundances (C/O ratio), and the **pulsational parameter** pulsation period P and amplitude Δu.

The effects of LMC metallicity

Hydrodynamic structure

The inner part of the hydrodynamic structure is characterized by a dust-free atmospheric region with an exponential density decrease (Fig. 1). The density structure maybe influenced by a pressure inversion ($r \approx 1.35\,R_0$, Fig. 1) due to locally strong molecular opacities (dashed lines, Fig. 2). This inner region is disturbed by the interior pulsation. Resulting shock waves levitate time-dependently the atmosphere to radial distances where the temperature is low enough to allow an efficient dust formation ($r \approx 3.5\,R_0$, Fig. 1). This transition region between the atmosphere and the circumstellar envelope, the *dustosphere* (greek: *Kornioktosphere*), is determined by the radiation pressure on newly formed dust and the correspondingly amplified shock waves.

The small efficiency of dust formation for LMC metallicities causes the models to evolve only very slowly. Matter falls inward (green

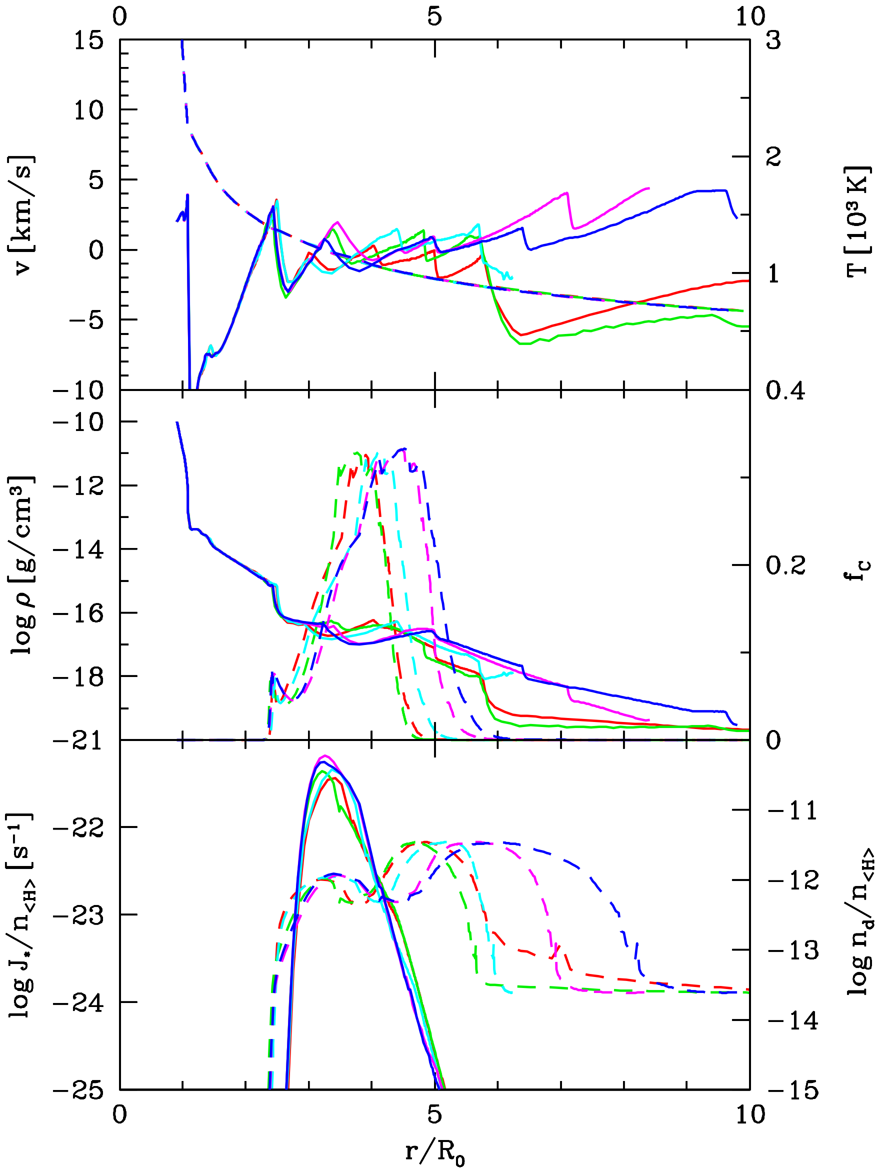

Figure 1: Hydrodynamic model structures for subsequent instants of time for a LMC carbon-rich AGB star dustosphere: red - t=145 P; green - t=148 P; cyan - t = 151 P; magenta - t = 154 P; blue - t = 156 P.
Model parameter: $T_\star = 3000$K, $L_\star = 10^4 L_\odot$, $M_\star = 1 M_\odot$, C/O=1.8, $\Delta u = 2$km s^{-1}, $P = 650$d.

Upper Panel: velocity u [km s^{-1}], temperature T [10^3 K] **Middle Panel**: gas density $\log\rho$ [g cm^{-3}], degree of condensation f_c **Lower Panel**: solid - total acceleration ratio $\alpha^{\rm tot}$, optical depth $\log\tau_{\rm L}$

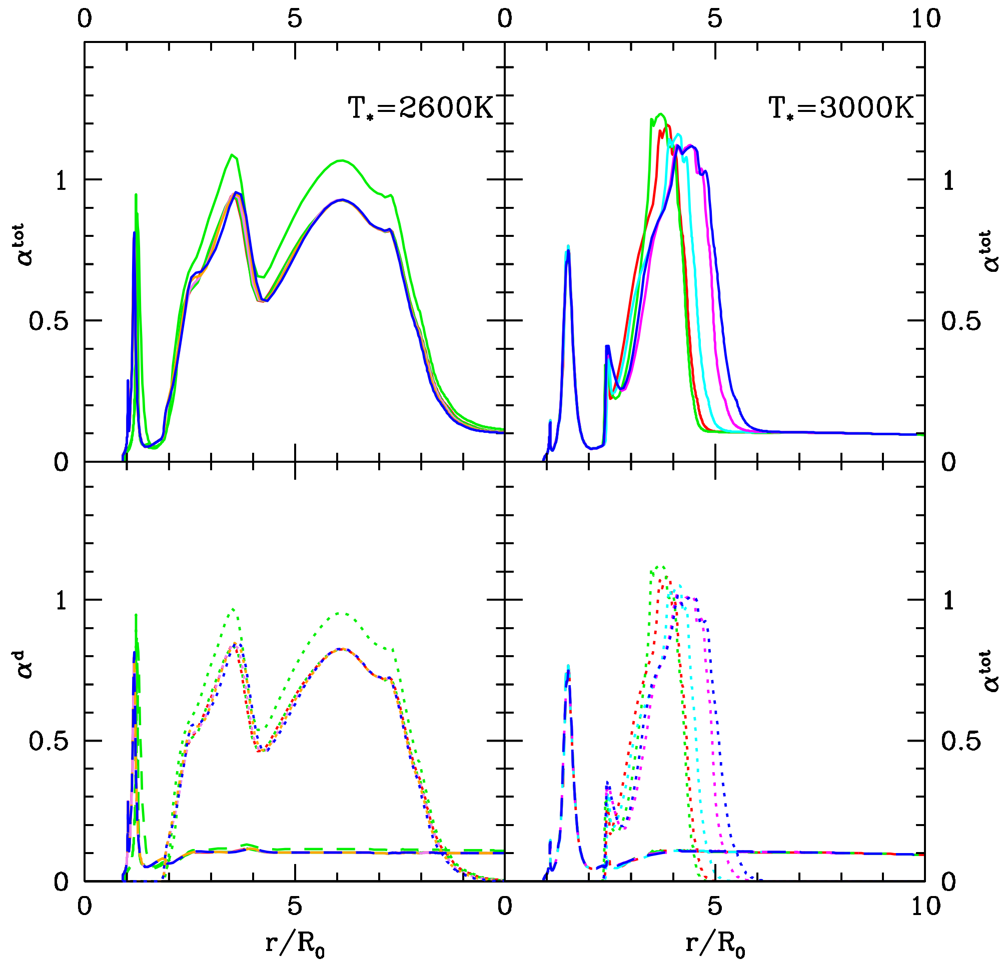

Figure 2: Radiative acceleration in two carbon-rich LMC models for subsequent instants of time.
Model parameter - left: $T_\star = 2600$K, $L_\star = 10^4 L_\odot$, $M_\star = 1 M_\odot$, C/O=1.8, $\Delta u = 2$km s^{-1}, $P = 650$d. (green - t=176 P; violet - t = 179 P; brown - t = 182 P; orange - t = 185 P)
Model parameter - right: $T_\star = 3000$K, $L_\star = 10^4 L_\odot$, $M_\star = 1 M_\odot$, C/O=1.8, $\Delta u = 2$km s^{-1}, $P = 650$d (color code like Fig. 1).

Upper Panels: total radiative acceleration $\alpha^{\rm tot} = a^{\rm tot}_{\rm rad}/g_\star = \alpha^{\rm d} + \alpha^{\rm g}$, **Middle Panels**: radiative acceleration due to dust $\alpha^{\rm d}$, **Lower Panels**: radiative acceleration due to gas $\alpha^{\rm g}$

curve, Fig. 1) and outward acceleration due to $a_{\rm rad} > g_\star$ occurs not continuously but episodic (Fig. 2). Thereby, radiation pressure on the gas provides a necessary percentage to overcome the stellar gravity (green curves, l.h.s. Fig. 2). Nevertheless, the total radiative acceleration is sufficient to *slowly extent the shell which surrounds the star*. The models appear rather quasi-static over hundreds of years.

In contrast to the solar case, the dust is located mainly in a single shell around the star since the backwarming is not large enough to inhibits further dust nucleation.

Dust size distribution

The local dust size distribution is a direct consequence of the thermodynamic condition of the gas from which the dust forms. *Characteristic multiply peaked grain size distributions* (Fig. 3) result for each Lagrangian mass element representing the *time dependent dust formation history* since $T = T(t)$ and $\rho = \rho(t)$ (Fig. 1).

The largest amount of small particles is contained in the mass element at $\sim 3\,R_0$ (upper panel, Fig. 3) since this is the site the nucleation rate peaks. Also most of the largest particles (up to $\sim 0.5\mu$m) are found here since dust particles, accumulated here by various infall events, continue to grow (green curve Fig. 1 and r.h.s. Fig. 2).

The influence of newly formed dust, i.e. the smallest particles, decreases with increasing distance from the star (lower panels, Fig. 3). Here, the local size distribution is determined mainly by the process of dust growth in an outward accelerated mixture of dust and gas. Since most of the condensible material is already consumed in this region, a large number of intermediate sized particles is present.

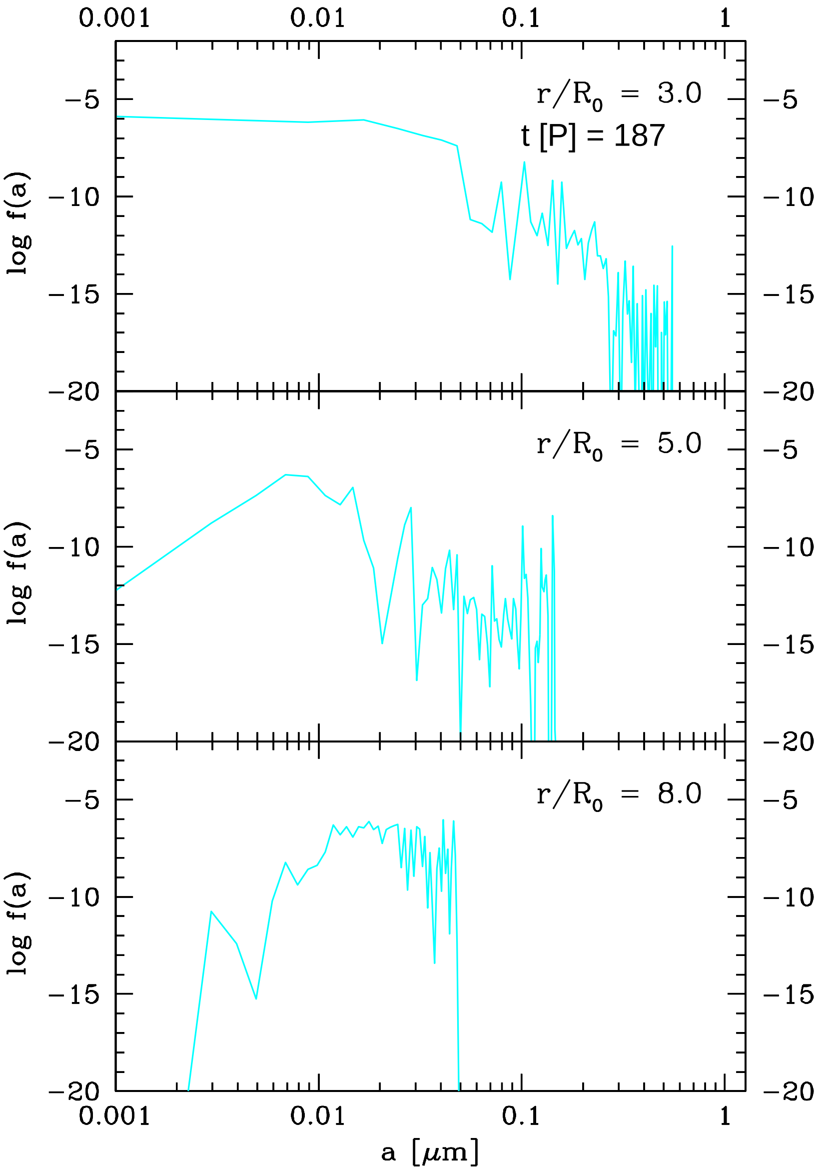

Figure 3: Grain size distributions of Lagrangian mass elements at different radial positions. **Model parameter:** $T_\star = 2600$K, $L_\star = 10^4 L_\odot$, $M_\star = 1 M_\odot$, C/O=1.8, $\Delta u = 2$km s^{-1}, $P = 650$d.

Wind properties

Wind properties like a mean mass loss rate $\langle \dot{M} \rangle$, a mean outflow velocity $\langle v_\infty \rangle$ and a mean dust-to-gas ratio $\langle \rho_{\rm dust}/\rho_{\rm gas} \rangle$ are difficult to define because of the quasi-static shell structure. They have to be considered with care but give an insight in general features of the LMC models (Fig. 4). Considering the time means $\langle \ \rangle_t$ at various radial positions, one observes:

- $\langle \dot{M} \rangle_t$, $\langle v_\infty \rangle_t$, and $\langle \rho_{\rm dust}/\rho_{\rm gas} \rangle_t$ vary depending on the radial distance from the star (Fig. 4).
- Dust containing regions show the largest values for $\langle \dot{M} \rangle_t$, $\langle v_\infty \rangle_t$, and $\langle \rho_{\rm dust}/\rho_{\rm gas} \rangle_t$.
- $\langle \dot{M} \rangle_t$ and $\langle \rho_{\rm dust}/\rho_{\rm gas} \rangle_t$ drop with increasing distance from the star.
- Locally, $\langle v_\infty \rangle_t < 0$ since low density material can fall inward for a long time but only few strong mass loss events suffice to push the shell a little bit further outward.

Table 1 contains the radial mean values (horizontal lines, $\langle \ \rangle_{t,r}$) of the time means depicted in Fig. 4. Comparing the values for different dust extinction data shows the largest effect in $\langle v_\infty \rangle_{t,r}$ and $\langle \rho_{\rm dust}/\rho_{\rm gas} \rangle_{t,r}$. This compares well with the results of Fleischer et al. (1999) and Andersen et al. (1999) for solar metallicities. However, the time means at various radial positions (Fig. 4) deviate more for the low temperature model ($T_\star = 2600$ K) and the differences due to the dust extinction data appears also for $\langle \dot{M} \rangle_t$.
The radial time-averaged values of $\langle \dot{M} \rangle_{t,r}$ and $\langle v_\infty \rangle_{t,r}$ derived from the LMC models presented so far deviate largely from the values of a solar metallicity star (Helling et al. 2000a). $\langle \rho_{\rm dust}/\rho_{\rm gas} \rangle_{t,r}$ is much

	Stellar Parameter					**Pulsation Parameter**		
#	$T_\star$ [K]	$L_\star$ [$L_\odot$]	$M_\star$ [$M_\odot$]	$\epsilon_{\rm el}$	C/O	P [d]	Δu [$\rm km\,s^{-1}$]	Data
1	2600	10^4	1	LMC	1.8	650	2	GSD
2	2600	10^4	1	LMC	1.8	650	2	Preib
3	3000	10^4	1	LMC	1.8	650	2	GSD
4	3000	10^4	1	LMC	1.8	650	2	Preib
5	3000	10^4	1	solar	1.8	650	2	GSD
6	3000	10^4	1	solar	1.8	650	2	Preib

	Resulting Quantities			
#	$\langle \dot M \rangle_{t,r}$ [$M_\odot$/yr]	$\langle v_\infty \rangle_{t,r}$ [km/s]	$\langle \rho_{\rm dust}/\rho_{\rm gas} \rangle_{t,r}$	Data
1	$6.0\,10^{-10}$	-0.58	$0.2\,10^{-3}$	GSD
2	$-1.6\,10^{-10}$	0.047	$0.46\,10^{-3}$	Preib
3	$7.2\,10^{-10}$	-0.42	$0.07\,10^{-3}$	GSD
4	$2.3\,10^{-10}$	-0.35	$1.1\,10^{-3}$	Preib
5	$4.4\,10^{-8}$	10.2	$0.046\,10^{-3}$	GSD
6	$8.4\,10^{-7}$	24.3	$1.7\,10^{-3}$	Preib

Table 1: Wind properties for LMC and solar circumstellar dust shells taking into account two data sets for the dust extinction. $\langle \dot M \rangle_{t,r}$, $\langle v_\infty \rangle_{t,r}$, and $\langle \rho_{\rm dust}/\rho_{\rm gas} \rangle_{t,r}$ are radial means of the time means at various radial distances depicted in Fig. 4.

less affected but smaller than the solar value.
However, present observations indicate that the mass loss rate of LMC AGB-stars does not differ significantly from a solar metallicity AGB-star but the dust-to-gas ratio is smaller (Wood et al. 1992, van Loon et al. 2001).

Conclusions

- Present models of LMC dustospheres develop a rather quasi-static structure (i.e. long hydrodynamical time scales) where the dust is only present in a unique shell. New dust is formed continuously at the inner edge of this shell which slowly extends.

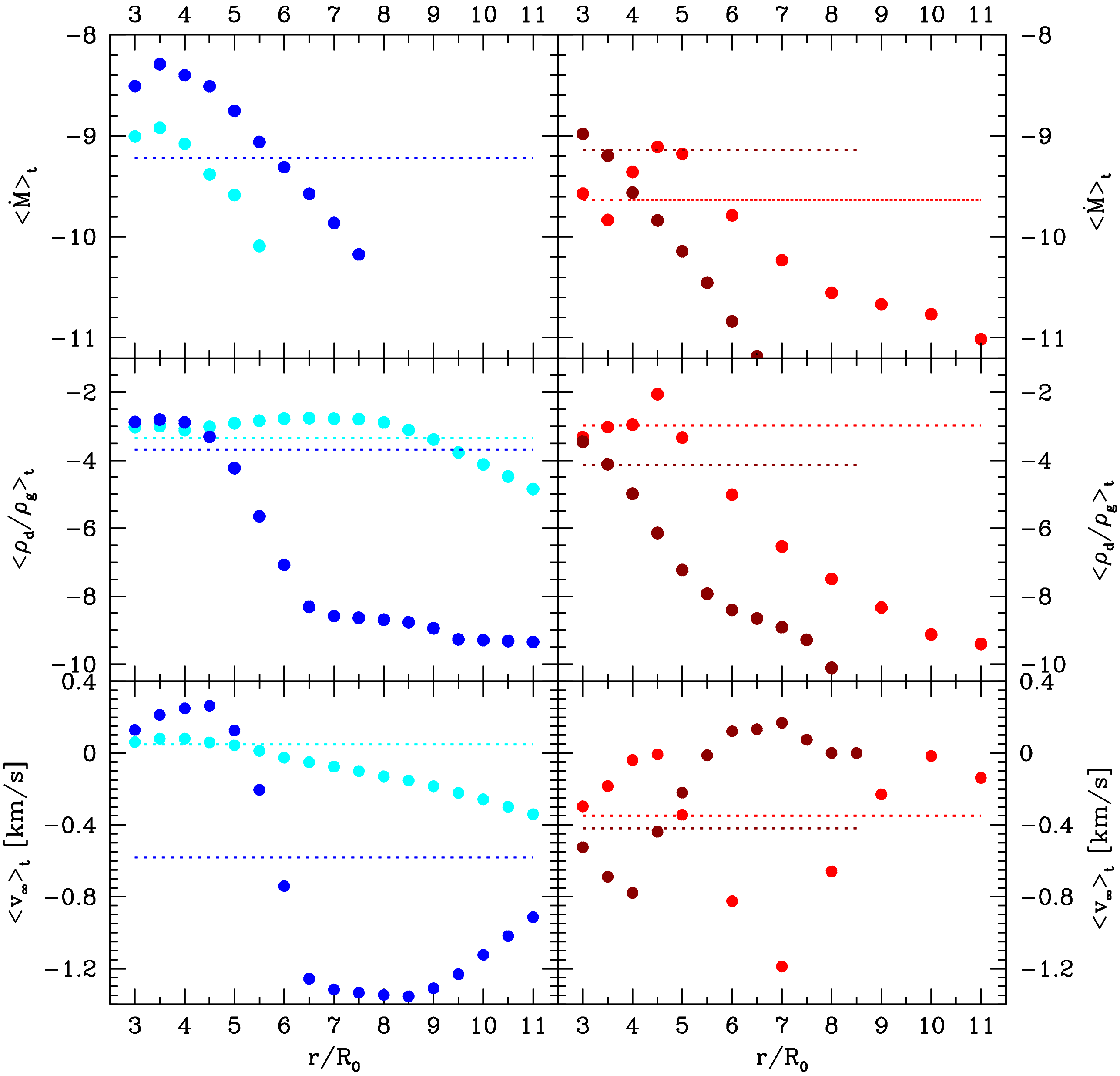

Figure 4: Time mean values of $\langle \dot{M} \rangle$, $\langle v_\infty \rangle$, $\langle \rho_{\rm dust}/\rho_{\rm gas} \rangle$ taken over 40 Periods ($\approx 70\,$yr) at various radial distances r. The horizontal dotted lines indicate the radial mean values of the time means (dots). Light colors represent Preibisch data for the dust extinction; dark colors the Gail & Sedlmayr (1985) temperature fit.
Model parameter: blue colors: $T_\star = 2600$K (l.h.s), red colors: $T_\star = 3000$K (r.h.s.); else: $L_\star = 10^4 L_\odot$, $M_\star = 1 M_\odot$, C/O=1.8, $\Delta u = 2$km s^{-1}, $P = 650$d.

- The decrease of the metal abundance significantly lowers the amount of dust formed and thereby causes a considerable reduction of the mean mass loss rate and mean outflow velocity compared to solar metallicity stars. In contrast, the mean dust-to-gas ratio decreases only slightly.

Our results suggest that the metal content of a LMC gas in the extended atmosphere of an AGB star (*dustosphere*) is too low to efficiently drive a wind by radiation pressure on dust grains alone. An additional driving mechanism – different from those already included in the models (pulsation, radiation pressure on dust and/or molecules) – possibly exists.

Acknowledgment: The work has been supported by the DFG (grant Se 420/19−1, 2) and the PROCOPE program (grant D/9822849 DAAD).

References

Andersen, A. C., Loidl, R., Höfner, S., 1999, A&A 349, 243
Fleischer A. J., Gauger A., Sedlmayr E., 1992, A&A 266, 321
Fleischer A. J., Winters, J. M., Sedlmayr E., 1999, IAU Symp. 191, eds. Le Bertre, T. et al. , 187
Gail H.-P., Sedlmayr E., 1985, A&A 148, 183
Gail H.-P., Sedlmayr E., 1988, A&A 206, 153
Gauger A., Gail H.-P., Sedlmayr E., 1990, A&A 235, 345
Hashimoto O., 1995, ApJ 442, 286
Helling Ch., Arndt M., T.U., Sedlmayr E., 2000a, AG Abstr. Ser. 17, 55
Helling Ch., Winters J. M., Sedlmayr E., 2000b, A&A 358, 651
Preibisch T., Ossenkopf V., Yorke H. W., Henning T., 1993, A&A 279, 577
Unno W., Kondo M., 1976, PASJ 28, 347
Unno W., Kondo M., 1977, PASJ 29, 693